

Polymer–Metal Schottky Contact with Direct-Current Outputs

Hao Shao, Jian Fang, Hongxia Wang, Liming Dai, and Tong Lin*

Conversion of mechanical energy into electricity is an important process widely used for power generation.^[1] Over centuries, large mechanical energies from steam flow, wind, and falling water have been converted into electrical power based on electromagnetic induction. Small mechanical energies associated with body movements, muscle contractions, rotation of vehicle tires, and rainfall, to name a few, exist everywhere.^[2] Harvesting these seemingly small energies into electricity to charge personal electronics is highly desirable, particularly for those with whom being charged by an alternating current (AC) line cord and/or a heavy battery are difficult (e.g., athletes, soldiers in the field).

Indeed, small mechanical energies have been harvested into electricity using miniaturized electromagnetic devices (or generators)^[3] and piezoelectric converters.^[4] Recently, other innovative mechanical energy to electricity conversion mechanisms have also been reported, for example, ionization of a polymer gel under mechanical deformation to generate electric signals of few millivolts,^[5] triboelectric generation of large voltage outputs,^[6] and electric energy generation simply by bringing two metals with different work functions together.^[7] However, most of the devices reported so far produce a low output current density, though some of them show large voltage outputs. Large current density is necessary to provide sufficient power to run a device for various practical applications, which should also open up avenues for miniaturizing the generators to be integrated into utilizing devices for self-powered miniature medical robots, for instance.^[8]

Most of the existing technologies for harvesting small mechanical energy can only produce alternating current outputs. Rectification is needed to produce direct current (DC) power before use. This not only reduces the overall energy conversion efficiency but also increases complexity and difficulty in miniaturizing the generator system. Self-rectified energy harvesters that can directly produce DC outputs without extra rectifying are highly promising. Piezoelectric DC generators have been reported based on oriented ZnO nanomaterials

(e.g., aligned nanowires, nanorods, and nanosheets) by forming Schottky contact between the ZnO nanomaterials and an electrode to regulate the charge movement.^[9] However, those devices typically have a low power output and also require precisely control of the preparation process. Besides, DC outputs have also been reported for triboelectric generators with multiple electrification pairs to periodically switch charging directions (see a summary of DC generators in the Supporting Information, Table S1).^[10]

Conducting polymers, such as polypyrrole (PPy), have demonstrated for mechanical-to-electrical energy conversion.^[11] Previous reports on mechanical energy harvesting involving PPy are often based on interaction with an electrolyte solution.^[12] The minute voltage output (e.g., 0.28 mV) and use of electrolyte solution make these devices unsuitable to be integrated into solid-state devices (e.g., wearable electronics). As far as we are aware, however, electric generation from mechanical deformation of a dry, freestanding PPy without electrolyte has not been reported to date.

Here, we have found that a freestanding PPy thin film (plate of 1–2 mm in thickness) under compression can generate a DC power with a current density as high as 62.4 $\mu\text{A cm}^{-2}$ and voltage of 0.7 V. We have further demonstrated that the electric energy thus generated can be directly stored into a capacitor without rectification to power electronic devices, as exemplified by lighting up a commercial light-emitting diode (LED) (vide infra).

In a typical experiment, PPy was synthesized using FeCl_3 as oxidant, and PPy plates (diameter: 13 mm; thickness: 1.44 ± 0.10 mm) were fabricated by mechanically pressing the PPy powders in the same manner as FTIR (Fourier transform infrared spectroscopy) KBr plates were made. **Figure 1a** shows a typical digital image for the as-prepared PPy plate. Scanning electron microscopy (SEM) images given in Figure S1 of the Supporting Information shows a typical globular morphology for PPy.^[13]

To measure the mechanical-to-electric conversion of the PPy plate, we used an aluminum foil and a gold sheet as electrodes and devised the electrical circuit, as shown in Figure 1b. The gold sheet was supported by a dense polyethylene terephthalate (PET) film of the same size. During the test, the PPy plate was mounted on the Al electrode, whereas the Au electrode was laminated to a nonconductive PET film and fixed to a movable load. The circuit is connected just during compressive impact of the PPy plate by the PET/Au-load. By moving up-and-down the gold electrode with the load, the PPy plate was compressed and decompressed to generate electric signals.

Figure 1c,d shows the voltage and current outputs, respectively, when the device was compressed to a strain up to

H. Shao, Dr. J. Fang, Dr. H. Wang, Prof. T. Lin
Institute for Frontier Materials
Deakin University
Geelong, VIC 3216, Australia
E-mail: tong.lin@deakin.edu.au
Prof. L. Dai
Center of Advanced Science and Engineering
for Carbon (Case4Carbon)
Case Western Reserve University
Cleveland, OH 44106, USA



DOI: 10.1002/adma.201504778

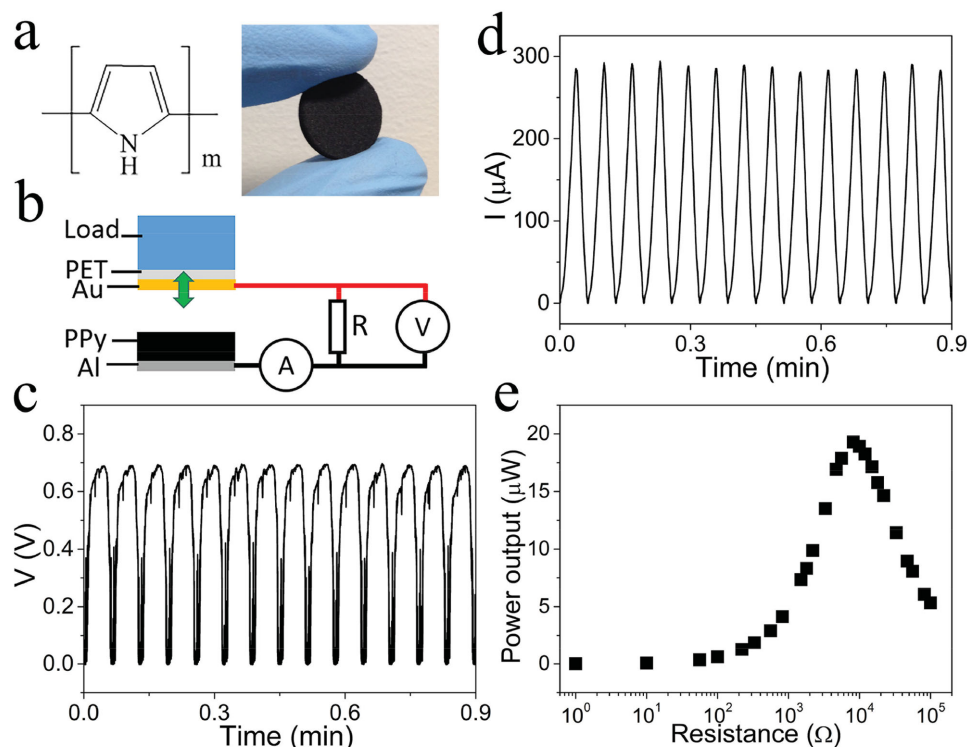


Figure 1. a) Chemical structure of PPy and digital image of the PPy plate (diameter: 13 mm); b) circuit (forward connection) for measurement of electrical outputs under strain; c,d) typical voltage and current outputs from a PPy plate under repeated compressive deformation (strain level: 10.4%; compression speed: 0.08 mm s^{-1} ; frequency: 0.27 Hz); e) relationship between the output power and the external load resistance (PPy plate thickness: $1.44 \pm 0.10 \text{ mm}$).

10.4% at a speed of 0.08 mm s^{-1} and then decompressed at the same speed. As can be seen, the peak current reaches up to 290 μA (current density 218.6 μA cm^{-2} , Figure 1d) at a peak voltage of 0.7 V (Figure 1c). The voltage and current outputs can be generated repeatedly over more than thousands of compression–decompression cycles as the 10.4% strain is within the elastic deformation of the PPy plate (see Supporting Information, Figure S2). Compared to various reported energy harvesting devices (see Supporting Information, Tables S1 and S2), our PPy-based energy harvesting unit shows a much higher current density, though voltage output is relatively low (0.7 V).

The power (P) outputs at different external resistances were calculated by the equation: $P = I^2 R$, where I is the peak current at the corresponding external resistance (R). Figure 1e shows the output power as a function of external load resistance from 1 Ω to 0.1 MΩ (see Supporting Information, Figure S3 for the I – R and V – R). The output power initially increased with increasing the external resistance to reach a maximum value of 0.15 W m^{-2} at 8.2 kΩ , and then decreased with further increase in the R value. It is known that an energy device shows a maximum P value when it works at an external resistance equivalent to the internal resistance.^[14]

To gain further insights into the mechanical energy–electricity conversion by the PPy plate, we employed different strain–time functions. Figure 2a shows the response of electrical outputs to a triangle compression–decompression strain cycles. As can be seen, the device voltage and current outputs

show a synchronous response to the compression under a periodic compression at a crosshead speed of 0.08 mm s^{-1} to the maximum strain of 10.4%; both voltage and current increase with increasing the strain value. However, the electric outputs responded to the strain in a nonlinear manner. The rates of voltage and current increases for the strain change from 0% to 5% were much lower than those for the strain change from 5% to 10%. Once the strain was removed, the outputs dropped to zero spontaneously.

When the PPy plate was pressed and held for certain period of time and then decompressed to the natural state, the electrical output profile changed with the duration (t_1) of holding the plate at certain strain. As shown in Figure 2b, both voltage and current decay slowly over several minutes even if the strain is kept at 10.4%. Once the strain is released from the PPy plate, however, both the outputs drop to zero immediately (Figure 2b). This differs significantly from conventional piezoelectric materials in which the electrical outputs decay very rapidly to zero even if the material is kept at the deformed state. The observed unique mechanical–to–electric conversion responses were repeatable for many cycles.

We further investigated the effects of the PPy plate geometrical dimensions on the electric outputs. As seen in Figure 2c, the current output increases from 7 to 83 μA (current density from 38.9 to 62.4 μA cm^{-2}) when the PPy plate area increases from 0.18 to 1.33 cm^2 while keeping the plate thickness unchanged. However, the voltage output remained almost the same (Figure 2c). Similarly, changing the plate thickness while

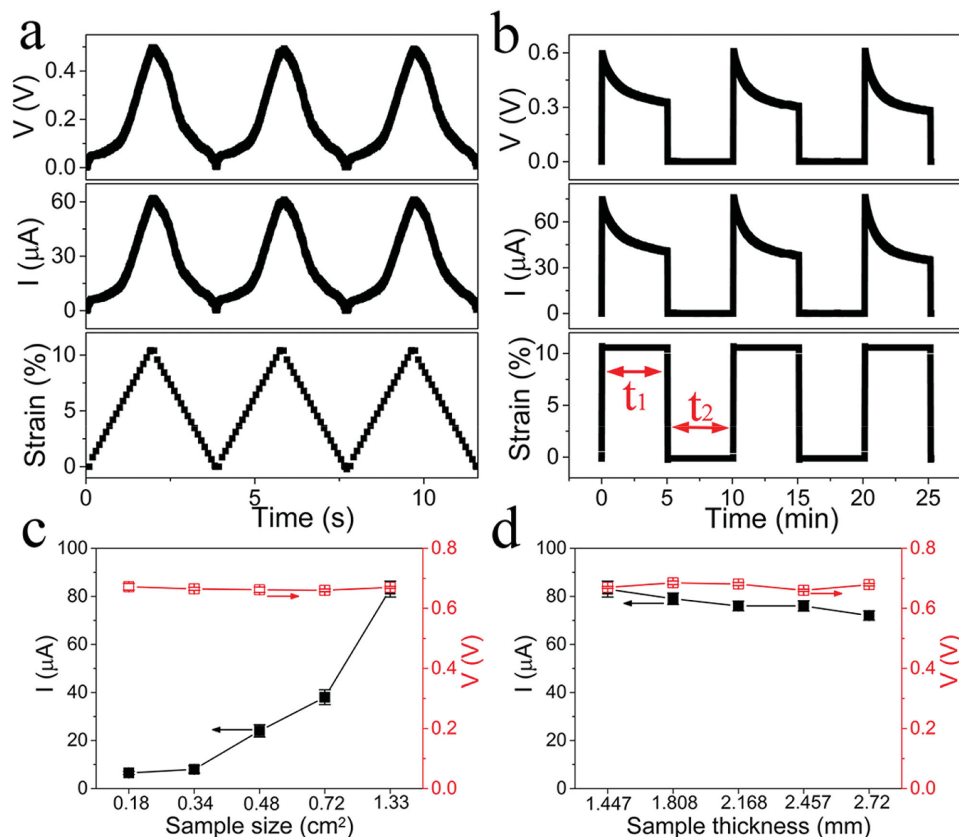


Figure 2. a) Electrical outputs of PPy plate as a function of strain change. b) Electrical outputs of PPy plate at a given compression condition (pressing time $t_1 = 300\text{s}$, $t_2 = 300\text{s}$; external load: $8.2\text{ k}\Omega$). c,d) Effect of plate size and thickness on electrical outputs (strain = 10.4%).

keeping the PPy plate diameter the same only changed the current output to a certain extent but had little effect on the voltage output. This is presumably due to the effect of internal resistance on the current output. Increasing the plate thickness or decreasing the area leads to increase in the internal resistance, hence reducing the current output.

We also noted that the impact side had little influence on the electric outputs. No matter which electrode was connected to the traveling load for compression, the PPy device generated the same level of electrical signals under the same strain (Supporting Information, Figures S12–S14). In addition, the electrical outputs were not affected by the electrode-PPy connection modes. When both electrodes are connected constantly to the PPy plate (Supporting Information, Figure S13a), the device shows similar electric outputs to those from the device with one of the electrodes discontinuously connected the PPy plate, as shown in Figure 1b. When the connection reversed, the output DC voltages reversed the polarity (Supporting Information, Figure S14).

To investigate the mechanism for the novel mechanical-to-electric energy conversion, we measured the I - V curve and electrical impedance spectrum (EIS) of the Au/PPy/Al device. As shown in Figure 3a, a nonlinear I - V curve with a Schottky diode feature is observed on the device in both gentle contact (1% strain level, to ensure the electric connection) and compressed states with a stronger rectifying effect for the device

under a compressive strain. From the Nyquist plots (Supporting Information, Figure S15), we estimated the internal electrical resistance of the device after the compression test to be approximately $8.3\text{ k}\Omega$, which is very close to that established from Figure 1e ($8.2\text{ k}\Omega$).

The rectifying effect indicates that a Schottky contact should exist within the device. To find out the Schottky contact, we examined devices with the same type of metal electrodes on both sides of PPy the plate (i.e., Au/PPy/Au and Al/PPy/Al). As shown in Figure 3b, a linear I - V characteristic is observed on the Au/PPy/Au device, indicating an Ohmic contact between the Au and PPy plate with an electrical resistance as low as $80\ \Omega$ (Figure 3b). For the Al/PPy/Al device, a nonlinear I - V relationship was observed with an electrical resistance as high as $12\text{ k}\Omega$, calculated based on the linear segment (Figure 3a). This suggests that Schottky contact should form between PPy and Al. Schottky contact between PPy and Al^[15] and Ohmic contact between PPy and Au^[16] have been reported previously. Our study was in good accordance with these reports.

For comparison, we also tested the mechanical-to-electrical conversion response of the Au/PPy/Au and Al/PPy/Al devices. As shown in Figure 3c, no electrical generation is observed on the Au/PPy/Au device under compression, but uneven positive and negative outputs with weak voltage output peaks of average around 0.1 V were generated on the Al/PPy/Al device under compressive impact (also see current output in Supporting

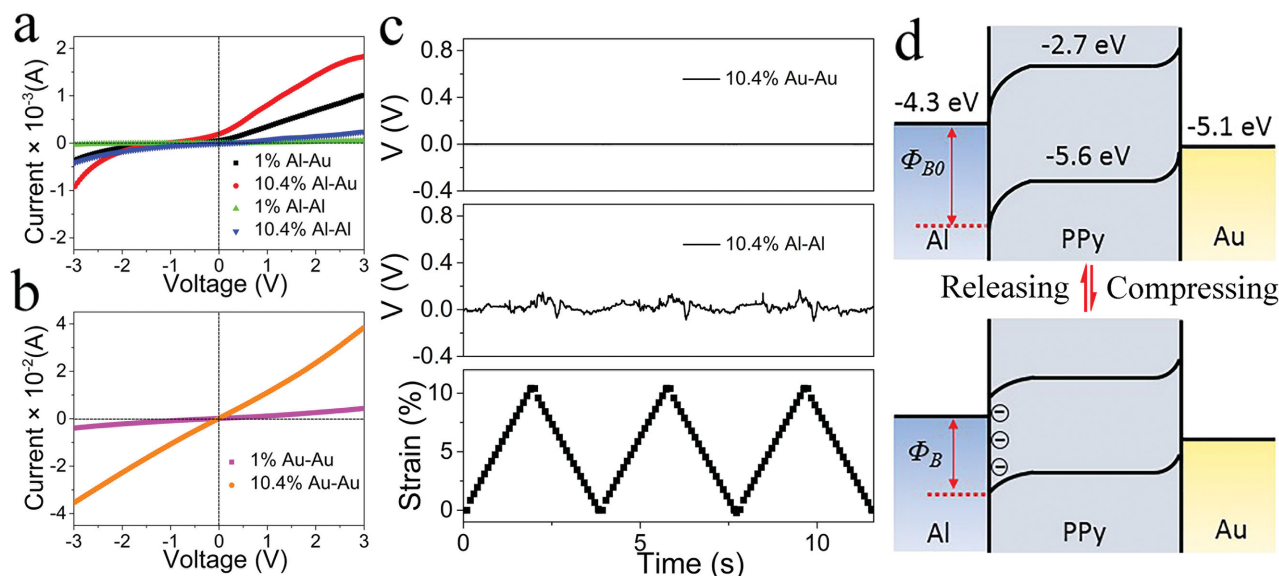


Figure 3. I–V characteristics of the a) Au/PPy/Al, Al/PPy/Al and b) Au/PPy/Au devices at gentle contact (strain: 1%) and compressed (strain: 10.4%) states. c) Voltage response of Al/PPy/Al and Au/PPy/Au devices under compressive strain (strain level: 10.4%, compression speed: 0.08 mm s⁻¹). d) Proposed energy band diagram of the Al/PPy/Au device at freestanding state and under compressive strain.

Information, Figure S17). However, the output voltage from the Al/PPy/Al device is not only significantly lower than that of the Al/PPy/Au counterpart but also in an AC mode. These results suggest that single Schottky contact in the Al/PPy/Au device plays a critical role in conversion of mechanical energy into DC power.

PPy is a p-type semiconductor with a LUMO and HOMO energy level of -2.7 and -5.6 eV, respectively.^[17] Metals Al and Au have a work function of 4.06–4.26 and 5.1–5.47 eV, respectively. Figure 3d illustrates the energy band diagram for the Al/PPy/Au device. The Al-PPy Schottky contact leads to electron flow to the metal side. The saturation current density of the Al/PPy/Au device can be estimated by equations^[15b,18]

$$J = J_0 \exp \frac{eV}{kT} \quad (1)$$

$$J_0 = A^* T^2 \exp \left(-\frac{\phi}{kT} \right) \quad (2)$$

where A* is the effective Richardson's constant, ϕ is the effective barrier potential, T is the absolute temperature, k is the Boltzmann constant, and V is the applied voltage. The barrier potential under compressive strain can be thus estimated based on Equation (1) as

$$\phi_{\text{strain}} = \phi_{\text{non-strain}} - kT \ln \left(\frac{J_{\text{strain}}}{J_{\text{non-strain}}} \right) \quad (3)$$

Here J_{strain} and $J_{\text{nonstrain}}$ are the current density at the same voltage in the linear part of the I–V curve. Since $J_{\text{strain}} > J_{\text{nonstrain}}$, the barrier potential under strain (ϕ_{strain}) is smaller than that at nature state ($\phi_{\text{nonstrain}}$). Such a reduction in the barrier potential would facilitate the movement of electrons from PPy to Al.^[15b,19]

The physical compression also increases charge density in the PPy plate because of the decreased volume. If the metal electrodes are not deformed under such a compressive impact, the increased charge density in the PPy together with the reduced interfacial barrier potential would allow more electrons move to the Al side. As a result, the potential difference increases. The Schottky diode plays a role in directional transfer of electrons, resulting in a DC output.

We also measured the effect of compression on the through-thickness resistance of the PPy plate. The resistance was found to decrease with increasing the strain value. Once the strain was removed, the electrical resistance went back to the initial level (Supporting Information, Figures S4 and S5). The observed resistance changes can be attributed to the reversible effect of compression on the PPy chain packing. Under compression, the PPy packing density increased with the intermolecular chain distance decreased, leading to an enhanced conductivity (Supporting Information, Figure S4).

It is known that frequent contact between two different materials could cause triboelectric charging. Energy devices based on triboelectric effect can generate a peak voltage output as high as 1163 V.^[20] In our case, the compressive impact between PPy plate and metal electrode during mechanical energy-to-electricity conversion might involve a triboelectric contribution. To examine the role of triboelectric effect, we prepared a device using two PPy plates from the same batch of PPy. By closely connecting an Au electrode onto one side of a PPy plate and an Al electrode onto one side of a separate PPy plate, and then making the PPy sides of the two plates to contact each other during compression, the triboelectric contribution can be eliminated. We noted that this Au/PPy/PPy/Al device can generate a similar voltage output but slightly lower current output (Supporting Information, Figure S19), when compared to the device made of single PPy plate (i.e., Au/PPy/Al) with regular PPy-metal connection/disconnection during compression

(Supporting Information, Figure S19). Triboelectric contribution can also be eliminated using closely packed Au/PPy/Al devices with constant PPy-electrode connection (see the result in Supporting Information, Figure S13). These results indicate that the mechanical energy-to-electricity conversion of our Au/PPy/Al is not based on triboelectric effect, though triboelectricity could contribute to electric output at certain conditions.

Therefore, the electric generation of our PPy/metal device under strain could come from three main aspects: (1) built-in Schottky contact with the metal, (2) strain-induced decrease in barrier potential of the Schottky contact allowing extra electron transfer to the metal side, and (3) increased electron density and reduced resistance in PPy under compression. The DC power originates from a switching process. However, the actual mechanism for the generation of a large electric circuit has yet been clear at this stage, which warrants a continuous investigation to clarify this fundamental issue.

To examine the effect of metal electrodes on power generation, we used other metals (e.g., stainless steel, Al alloy, and Cu) and ITO to replace Al and Au. We found that the device was able to generate DC output under compressive impact as long as a Schottky contact formed on one side of PPy plate, and an Ohmic contact formed on the other (see Supporting Information, Table S5). In addition, a similar DC energy generation feature was achieved for other types of conducting polymers, including polyaniline and polythiophene (Supporting Information, Figures S20 and S21). Therefore, the built-in Schottky barrier distinguishes our devices from the conventional mechanical-to-electrical energy harvesters, and the methodology developed in this study can be considered as a general platform technology for producing DC power from various metal/conducting polymer Schottky diodes under strain.

To demonstrate the potential applications for the energy generated from the Al/PPy/Au device, we used a capacitor to directly collect the electric output without using external

rectifier (Supporting Information, Figure S22). Figure 4a shows the voltage change of the capacitor charged by the working device. It took less than 20 s to charge a 220 μF capacitor to 0.7 V, while charging 1.0 and 2.2 mF capacitors to the same voltage took 2.5 and 7 min, respectively. By connecting 10 charged 2.2 mF capacitors in parallel, the stored electric energy was able to drive miniature electric motor and power commercial LED (Figure 4b, also see videos in Supporting Information). To further facilitate the practical use, we also prepared a coin-type mechanical energy-electricity conversion device based on the Al/PPy/Au plate by using the accessories for making coin batteries. Figure 4c shows a photo of the coin energy generator, along with the device structure. By finger tapping the device, electric signals generated (see the video in Supporting Information).

In summary, we have developed a novel concept of using single Schottky contact between a conducting polymer plate and a metal electrode to directly convert mechanical energy into DC electricity. The built-in Schottky barrier plays a key role in self-rectification. The electrical energy thus generated is sufficient to drive commercial electronic devices, as exemplified by commercial motor and LED diode. This novel DC electricity may open up new avenues for further fundamental research and experimental development of DC energy harvesting systems of practical significance.

Experimental Section

Materials: Iron(III) chloride hexahydrate ($\text{FeCl}_3 \cdot 6\text{H}_2\text{O}$) ($\geq 98\%$), pyrrole ($\geq 98\%$), 3,4-ethylenedioxythiophene (EDOT) (97%), and aniline ($\geq 99.5\%$) were purchased from Sigma-Aldrich and used as received.

Plate Preparation: PPy was synthesized using a vapor phase polymerization method. Briefly, FeCl_3 fine powder was placed in a glass dish in a vacuum chamber. The monomer was placed underneath the FeCl_3 plate. In vacuum, the monomer evaporated to fill the entire chamber, in which polymerization took place on FeCl_3 surface. Once the reaction started, the brownish FeCl_3 turned black. After 48 h reaction at room temperature, the black powder was added to water and stirred for 48 h to remove unreacted chemicals and any side product. The powder was then washed with distilled water for several times before drying in a vacuum oven at 60 $^\circ\text{C}$. After drying, the conducting polymer was ground manually into finer powder and then pressed into plates using a steel die (7.5 tonnes for 3 min).

Characterization: Surface morphology was observed under a SEM (Zeiss Supra 55VP). X-ray diffraction (XRD) patterns were obtained on a Panalytical X-ray diffractometer with Cu radiation of 1.54 \AA . The samples were scanned in the 2θ range of 10° – 80° with the step size of 0.05° . FTIR spectra were obtained on a Bruker Optics spectrometer in ATR mode. Raman measurements were performed on a Renishaw InVia Raman microscope equipped with a 514.5 nm laser. A 50 \times objective lens was used and the laser power was around 5 mW. XPS data were acquired using a Kratos AXIS Ultra (DLD) spectrometer equipped with a monochromated Al K α X-ray source (energy ≈ 1486.6 eV). Survey spectra were recorded at 1 eV per step and a pass energy of 160 eV while high-resolution spectra was performed at 0.1 eV per step and a pass energy of 20 eV. The pressure in the analysis chamber was maintained at about 3×10^{-9} Torr. Stress–strain curves were obtained on an Instron Universal Tensile Tester (model 5967), and the equipment was used to generate desired strain levels on the PPy plates. The electrical outputs were recorded by an e-Corder 401 electrochemistry working station, while the electrical resistance of the plate was measured by a Keithley 6514 electrometer. *I*–*V* curves and electrical impedance results were obtained using a CHI 760D electrochemical working station.

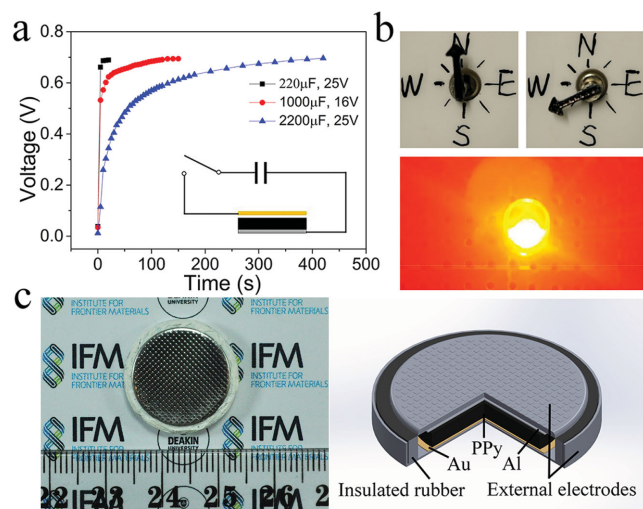


Figure 4. a) Voltage–time during charging of capacitors with an Au/PPy/Al device; Inset: the charge circuit. b) Pictures taken from video to show the rotation of a motor powered by a PPy plate and lighting of a commercial LED. c) A photo of coin generator and corresponding device structure.

Supporting Information

Supporting Information is available from the Wiley Online Library or from the author.

Acknowledgements

H.S. and J.F. contributed equally to this work. Funding support from ARC Future Fellow Grant (ARC FT120100135) is acknowledged.

Received: September 28, 2015

Revised: October 21, 2015

Published online: December 7, 2015

- [1] P. Breeze, *Power Generation Technologies*, 2nd ed., Newnes, Oxford 2014.
- [2] a) A. D. Kuo, *Science* 2005, 309, 1686; b) P. D. Mitcheson, E. M. Yeatman, G. K. Rao, A. S. Holmes, T. C. Green, *Proc. IEEE* 2008, 96, 1457; c) Z. Wang, *Nanogenerators for Self-Powered Devices and Systems*, Georgia Institute of Technology, SMARTech Digital Repository, Atlanta 2011.
- [3] L. Liao, P. C. Chao, J. Chen, W. Chen, W. Hsu, C. Chiu, C. Lin, *IEEE Trans. Magn.* 2009, 45, 4621.
- [4] a) A. J. Lovinger, *Science* 1983, 220, 1115; b) C. R. Bowen, H. A. Kim, P. M. Weaver, S. Dunn, *Energy Environ. Sci.* 2014, 7, 25; c) Z. L. Wang, J. Song, *Science* 2006, 312, 242; d) W. Wu, C. Pan, Y. Zhang, X. Wen, Z. L. Wang, *Nano Today* 2013, 8, 619; e) J. Fang, X. Wang, T. Lin, *J. Mater. Chem.* 2011, 21, 11088; f) J. Fang, H. Niu, H. Wang, X. Wang, T. Lin, *Energy Environ. Sci.* 2013, 6, 2196; g) H. Shao, J. Fang, H. Wang, T. Lin, *RSC Adv.* 2015, 5, 14345.
- [5] Y. Osada, J. P. Gong, *Adv. Mater.* 1998, 10, 827.
- [6] a) Z. L. Wang, *ACS Nano* 2013, 7, 9533; b) Z. L. Wang, *Faraday Discuss.* 2014, 176, 447.
- [7] A. Varpula, S. J. Laakso, T. Havia, J. Kyynarainen, M. Prunnila, *Sci. Rep.* 2014, 4, 6799.
- [8] D. Rus, M. T. Tolley, *Nature* 2015, 521, 467.
- [9] a) X. Wang, J. Song, J. Liu, Z. L. Wang, *Science* 2007, 316, 102; b) M. Y. Choi, D. Choi, M. J. Jin, I. Kim, S. H. Kim, J. Y. Choi, S. Y. Lee, J. M. Kim, S. W. Kim, *Adv. Mater.* 2009, 21, 2185; c) G. C. Yoon, K. Shin, M. K. Gupta, K. Y. Lee, J. Lee, Z. L. Wang, S. Kim, *Nano Energy Mater.* 2015, 12, 547.
- [10] a) Y. Yang, H. Zhang, Z. L. Wang, *Adv. Funct. Mater.* 2014, 24, 3745; b) C. Zhang, T. Zhou, W. Tang, C. Han, L. Zhang, Z. L. Wang, *Adv. Energy Mater.* 2014, 4, 1301798.
- [11] a) A. Bhattacharya, A. De, *Prog. Solid State Chem.* 1996, 24, 141; b) Y. Berdichevsky, Y. H. Lo, *Adv. Mater.* 2006, 18, 122; c) M. Ma, L. Guo, D. G. Anderson, R. Langer, *Science* 2013, 339, 186.
- [12] a) Y. Wu, G. Alici, J. D. W. Madden, G. M. Spinks, G. G. Wallace, *Adv. Funct. Mater.* 2007, 17, 3216; b) W. Takashima, K. Hayashi, K. Kaneto, *Electrochem. Commun.* 2007, 9, 2056.
- [13] J. Skodova, D. Kopecky, M. Vrnata, M. Varga, J. Prokes, M. Cieslar, P. Bober, J. Stejskal, *Polym. Chem.* 2013, 4, 3610.
- [14] J. Briscoe, N. Jalali, P. Woolliams, M. Stewart, P. M. Weaver, M. Cain, S. Dunn, *Energy Environ. Sci.* 2013, 6, 3035.
- [15] a) J. Unsworth, Z. Jin, B. A. Lunn, P. C. Innis, *Polym. Int.* 1991, 26, 245; b) K. Potje-Kamloth, *Chem. Rev.* 2008, 108, 367.
- [16] P. S. Abthagir, R. Saraswathi, *J. Appl. Polym. Sci.* 2001, 81, 2127.
- [17] M. Onoda, K. Tada, *Thin Solid Films* 2001, 393, 284.
- [18] M. Campos, F. Simoes, E. Pereira, *Sensors Actuators, B* 2007, 125, 158.
- [19] a) Q. Fu, Z. Zhang, L. Kou, P. Wu, X. Han, X. Zhu, J. Gao, J. Xu, Q. Zhao, W. Guo, D. Yu, *Nano Res.* 2011, 4, 308; b) X. Zheng, Z. Lang, W. Yijiao, W. Kangliang, D. Gang, K. Jinfeng, L. Xiaoyan, *Jpn. J. Appl. Phys.* 2014, 53, 04EN06; c) W. Wu, L. Wang, Y. Li, F. Zhang, L. Lin, S. Niu, D. Chenet, X. Zhang, Y. Hao, T. F. Heinz, *Nature* 2014, 514, 470.
- [20] Y. Zheng, L. Cheng, M. Yuan, Z. Wang, L. Zhang, Y. Qin, T. Jing, *Nanoscale* 2014, 6, 7842.